

# Synthesis and electron field emission of nanocrystalline diamond thin films grown from N<sub>2</sub>/CH<sub>4</sub> microwave plasmas

D. Zhou,<sup>a),b)</sup> A. R. Krauss, L. C. Qin, T. G. McCauley, and D. M. Gruen  
*Materials Science and Chemistry Divisions, Argonne National Laboratory, Argonne, Illinois 60439*

T. D. Corrigan and R. P. H. Chang  
*Department of Materials Science and Engineering, Northwestern University, Evanston, Illinois 60208*

H. Gnasler  
*Department of Physics, University of Kaiserslautern, D-67663 Kaiserslautern, Germany*

(Received 24 April 1997; accepted for publication 28 July 1997)

Nanocrystalline diamond films have been synthesized by microwave plasma enhanced chemical vapor deposition using N<sub>2</sub>/CH<sub>4</sub> as the reactant gas without additional H<sub>2</sub>. The nanocrystalline diamond phase has been identified by x-ray diffraction and transmission electron microscopy analyses. High resolution secondary ion mass spectroscopy has been employed to measure incorporated nitrogen concentrations up to  $8 \times 10^{20}$  atoms/cm<sup>3</sup>. Electron field emission measurements give an onset field as low as 3.2 V/μm. The effect of the incorporated nitrogen on the field emission characteristics of the nanocrystalline films is discussed. © 1997 American Institute of Physics. [S0021-8979(97)02821-1]

## I. INTRODUCTION

Nitrogen has been recognized as an important impurity in diamond, and the nature of its electronic states has been a central concern in elucidating the semiconducting properties of both natural and synthetically grown diamonds.<sup>1</sup> Although substitutional nitrogen in diamond is a deep donor impurity with a level at 1.9 eV below the minimum of the conduction band,<sup>2</sup> nitrogen impurities can affect the optical transparency,<sup>3</sup> the thermal conductivity,<sup>4</sup> and the electron field emission characteristics of diamond.<sup>5,6</sup> Incorporation of nitrogen impurities into chemical vapor deposit (CVD) diamond films has been extensively investigated by directly adding nitrogen to the reactant gas during the film deposition process.<sup>7,8</sup> However, substitutional doping of CVD diamond with nitrogen has proven extremely difficult, presumably because the reactant gas used for film growth is atomic hydrogen rich, which has a strong etching effect on any nondiamond phase deposition.

Because of their low (or negative) electron affinity and their chemical stability, diamond and its related materials have been intensively studied as cold cathode electron field emitters. Recently, field emission has been demonstrated from mesa-etched diodes using carbon ion implantation into *p*-type diamond substrates,<sup>9</sup> CVD polycrystalline diamond thin films,<sup>10</sup> and pulsed laser deposited diamondlike carbon thin films.<sup>11</sup> Due to its wide band gap, diamond has a very high electron resistivity. It is therefore difficult to transport electrons to the emitting surface, thus limiting the development of diamond based materials as cold cathodes for flat panel displays. Although *p*-type doping can greatly improve the conductivity of diamond, it has no effect on the emission characteristics, except that structural defects caused by the

doping process (such as ion implantation), which may provide some gap states, enhance the electron emission.<sup>12</sup> Unlike the doping impurities or dopant related defects (point defects), however, the density and the gap states provided by the structural (linear or planar) defects in the CVD diamond films are difficult to control. By contrast, *n*-type doped diamond films should be able to overcome these limitations and enhance electron field emission properties. Unfortunately, *n*-type doped diamond films have not been available up to now.<sup>13</sup>

In this article, synthesis of nitrogen-incorporated nanocrystalline diamond thin films and their electron field emission properties are reported. The films have been prepared by microwave plasma enhanced CVD with a mixture of CH<sub>4</sub> and N<sub>2</sub> as the reactant gas. The nanocrystalline diamond phase in the resulting films has been identified by x-ray diffraction (XRD) and transmission electron microscopy (TEM) as well as electron energy loss spectroscopy (EELS). High resolution secondary ion mass spectroscopy (SIMS) analysis (monitoring CN<sup>-</sup> negative secondary ions) reveals a high concentration of nitrogen with a uniform depth profile throughout the film. Electron field emission measurements show that the nitrogen impurities or nitrogen related defects strongly enhance the electron field emission from the films. Based on the microstructural characterization and the field emission measurement, the influences of nitrogen impurities on the electron field emission properties are discussed.

## II. EXPERIMENTS

The effects of nitrogen as an addition or impurity in the reactant gas on the properties of the resulting CVD diamond films have been extensively studied.<sup>14-17</sup> Up to now, nitrogen has not been successfully incorporated into diamond films to act as a donor impurity. In this study, a mixture of CH<sub>4</sub> (2 sccm) and N<sub>2</sub> (48 sccm) has been employed as the reactant gas for the microwave plasma enhanced CVD thin film preparation. *N*-type single crystal silicon wafers with

<sup>a)</sup>Electronic mail: dzhou@pegasus.cc.ucf.edu

<sup>b)</sup>Current address: Advanced Materials Processing and Analysis Center, Department of Mechanical, Material, and Aerospace Engineering, University of Central Florida, Orlando, FL 32816.

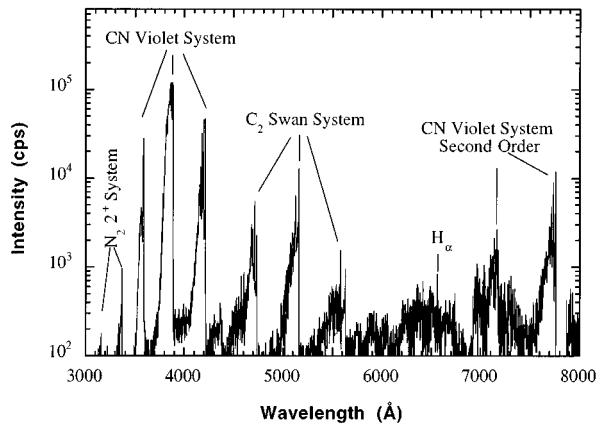


FIG. 1. An optical emission spectrum of  $N_2/CH_4$  plasma used for the film deposition.

$\langle 100 \rangle$  orientation were used as the substrates, and mechanical polishing with fine diamond powder ( $0.1 \mu\text{m}$ ) was employed to provide nucleation sites for film growth. During the deposition process, the substrate temperature, input microwave power, and total ambient pressure were kept under  $800^\circ\text{C}$ ,  $1100 \text{ W}$ , and  $35 \text{ Torr}$ , respectively. The films prepared in this work were one micrometer thick, as determined by using an *in situ* laser reflectance interferometer to monitor modulations of the surface reflectivity during the film growth.<sup>18</sup> In order to obtain some information on plasma chemistry, optical emission spectroscopy was employed to monitor the  $N_2/CH_4$  plasma. The characterization of the as-grown films was then carried out by using XRD, TEM, EELS, and high-resolution SIMS.

The electron field emission properties of the samples were investigated by the cold cathode electron field emission test apparatus. The anode with  $1.8 \text{ mm}$  in diameter was flat except for a slight rounding at the corners to eliminate sharp edges. The gap between the anode (probe) and the cathode (sample) was computer controlled via a stepping motor. The initial gap between the electrodes was determined by an optical microscope attached to a CCD camera and a TV monitor. Characteristics of emission current versus applied field were then obtained by scanning the applied potential between the electrodes from  $0$  to  $3000 \text{ V}$  with a series of increasing gap distances. The emission current was converted to a  $0\text{--}10 \text{ V}$  signal by an electrometer that was typically operated to provide maximum output for an emission current of  $10 \mu\text{A}$ . The cathode voltage was applied by an analog programmable  $5 \text{ kV}$  power supply under computer control, and the measured emission current was logged at each voltage. The measurements were carried out under a low  $10^{-8} \text{ Torr}$  ambient pressure.

### III. RESULTS AND DISCUSSION

Figure 1 shows an optical emission spectrum of the  $N_2/CH_4$  plasma used for the film deposition. As the labels in the spectrum indicate, the optical emission from the plasma consists mainly of the  $N_2$  second positive system, the CN violet system ( $B^2\Sigma - X^2\Sigma_v$ ), the  $C_2$  Swan system ( $d^3\Pi_g$

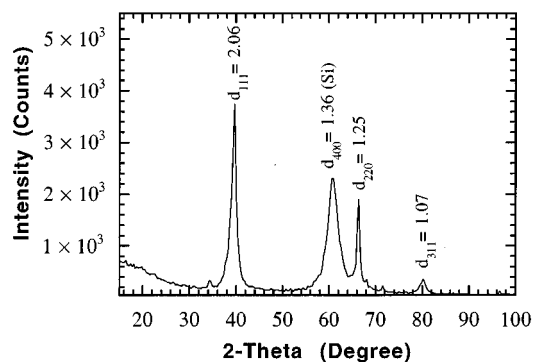


FIG. 2. The x-ray diffraction spectrum of the as-grown film showing the diffraction lines (111, 220, and 311) for cubic diamond. Note that the spectrum also consists of a Si {400} diffraction peak.

$-a^2\Pi_u$ ), and the CN second-order violet system. We have observed that the growth rate of the films is proportional to the density of  $C_2$  dimer in the plasma, but independent of the concentration of CN molecules. Therefore, the  $C_2$  dimer appears to be the major growth species from the  $N_2/CH_4$  plasma.  $C_2$  as a growth species for diamond film in  $\text{Ar-C}_{60}$  plasma was first proposed by Gruen *et al.*,<sup>19</sup> and details of the growth mechanism with  $C_2$  dimer have been discussed in the literature.<sup>20</sup>

The x-ray diffraction spectrum of the as-grown film is shown in Fig. 2. The diffraction peaks can be indexed on the basis of the cubic diamond structure (see the labels in Fig. 2) with no evidence of hexagonal stacking or a graphite phase. Note that the diffraction peaks are significantly broadened, meaning that the diamond crystals in the film have very small grain sizes. The silicon diffraction peak from {400} planes is due to the substrate. X-ray diffraction is not sensitive to noncrystalline phases, and thus no information on amorphous carbon is available with this method. Further characterization of the films has been conducted using TEM. Figure 3(a) shows a plane view TEM image, indicating that the film contains very fine grains with sizes ranging from  $10$  to  $30 \text{ nm}$ . The insert image shows a ring pattern from a selected area (over  $10 \mu\text{m}$  in diameter) electron diffraction, illustrating that the diamond grains have a random orientation. EELS was employed as a diagnostic for amorphous or disordered carbon with  $sp^2$  bonding. It is known that different carbon phases (graphite or amorphous carbon, and diamond) have very distinct  $K$ -shell absorption edge structures. Diamond has a single EELS feature with an onset at  $289 \text{ eV}$  due to its  $\sigma^*$  electronic states, while graphite or amorphous carbon has an additional EELS edge starting at  $284 \text{ eV}$ , owing to its lower-lying antibonding  $\pi^*$  states. Figure 3(b) shows an EELS spectrum of the nitrogen incorporated nanocrystalline diamond film acquired over an area of  $\sim 10 \mu\text{m}$  in diameter, displaying only an EELS edge at  $289 \text{ eV}$ , characteristic of diamond. No energy loss feature at  $284 \text{ eV}$  has been observed, suggesting a lack of amorphous or graphite phases in the film.

For conventional SIMS analysis, characterization of incorporated nitrogen in diamond thin films is difficult because of the interference of hydrocarbon masses with positive ni-

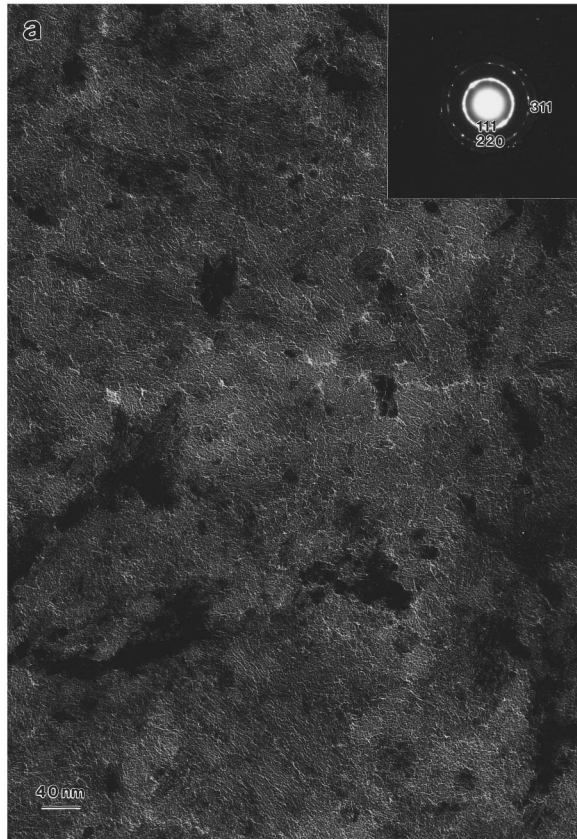


FIG. 3. (a) A plan view TEM image of the diamond thin film demonstrating that diamond grains have very fine sizes ranging from 10 to 30 nm. The insert image showing a selected area electron diffraction pattern; (b) EELS spectrum of the as-grown film displaying only  $K$  edge at 289 eV, characteristic of carbon with  $sp^3$  electron configuration.

nitrogen secondary ions (very low ion yield) and because of no stable negative nitrogen ions. In this study,  $CN^-$  negative secondary ions with a mass of 26.0031 amu have been measured by high resolution SIMS for the characterization of incorporated nitrogen.<sup>21</sup> A mass spectrum of the as-grown film shown in Fig. 4(a), illustrative of the nature of the SIMS data, demonstrates a  $CN^-$  secondary ion peak with a mass of 26.0030 amu. Figure 4(b) displays the depth profiles of carbon, nitrogen, and silicon through the film, illustrating that the concentration of the incorporated nitrogen in the as-grown nanocrystalline diamond thin film is as high as  $\sim 8 \times 10^{20}$  atoms/cm<sup>3</sup> with a uniform distribution through the

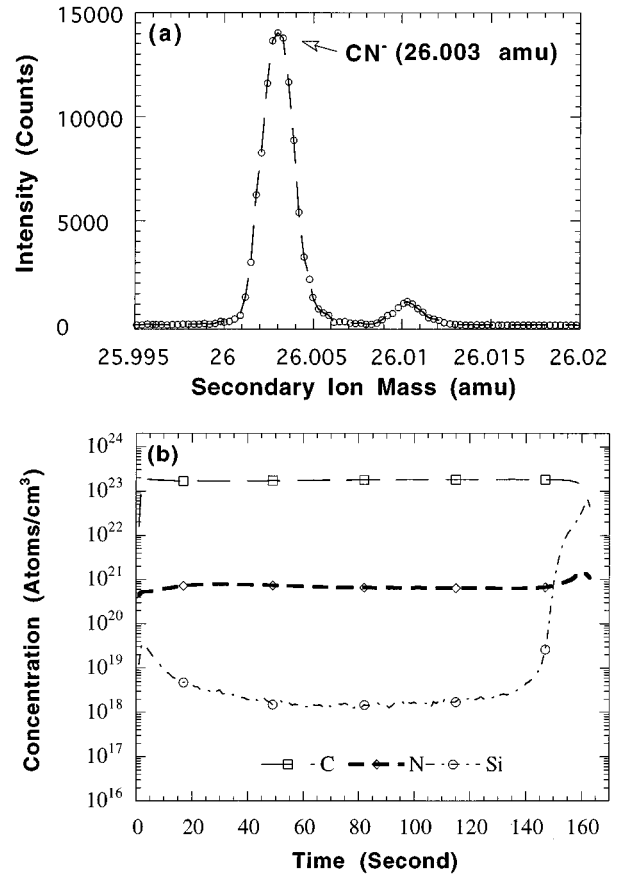


FIG. 4. High-resolution SIMS spectra of the as-grown film revealing the incorporation of nitrogen: (a) A high-resolution SIMS spectrum of the film demonstrating a  $CN^-$  secondary ion peak with a mass of 26.0030 amu; (b) Depth profiles of carbon, nitrogen, and silicon through the film which is 1  $\mu\text{m}$  thick.

film which is 1  $\mu\text{m}$  thick. Note that besides nitrogen, the film also contains significant amounts of hydrogen, which may be trapped at the grain boundaries to terminate the carbon dangling bonds. Oxygen impurity has also been observed in the film, which may be due to the Si substrate containing some  $SiO_2$  at the surface even after the mechanical polishing for seeding. All elements in the depth profiles were detected as negative secondary ions (under 14.5 keV  $Cs^+$  ion bombardment). The concentration scale is established using relative sensitivity factors derived from implantation standards. Note that  $1.8 \times 10^{23}$  atoms/cm<sup>3</sup> is used as the (average) carbon concentration of diamond for the calibration.

It is of interest to test the electron field emission properties of the films because the high concentration of incorporated nitrogen impurities or the nitrogen related defects may offer electron gap states, and thus enhance the electron field emission from the surface. Figure 5(a) shows plots of emission current density versus applied voltage with gap distances between the electrodes of 30, 130, and 230  $\mu\text{m}$ . These measurements demonstrate that for the nitrogen incorporated diamond film, the onset field for the field emission with a current of 4  $\mu\text{A}/\text{cm}^2$  when a 1.8 mm diam probe has been used is about 3.2 V/ $\mu\text{m}$ , while a field of  $\sim 6$  V/ $\mu\text{m}$  is required to obtain an emission current density of 0.4 mA/cm<sup>2</sup>. Fowler-Nordheim plots of  $\ln(J/F^2)$  vs  $1/F$  are shown in Fig.

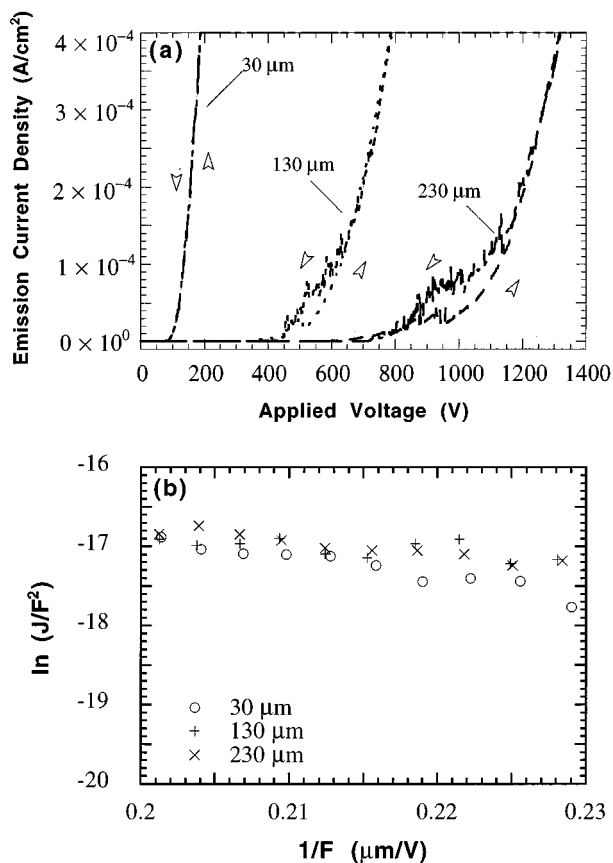


FIG. 5. (a) Plots of emission current density from the nitrogen incorporated nanocrystalline thin film vs applied voltage between the electrodes with different gaps. Arrows indicate the applied voltage increasing and decreasing cycles, respectively; (b) Fowler–Nordheim plots of  $\ln(J/F^2)$  vs  $1/F$  for field emission measurement at different gaps, where  $J$  is the emission current density ( $A/cm^2$ ) from the film and  $F$  is the applied electric field ( $V/\mu m$ ) between the electrodes.

5(b), where  $J$  is the emission current density ( $A/cm^2$ ) from the sample and  $F$  is the applied electric field ( $V/\mu m$ ). The plotted data for the measurements with three different gaps appear to fit a straight line supporting a Fowler–Nordheim tunneling mechanism.<sup>22</sup>

Previously, incorporation of high concentrations of nitrogen into CVD diamond thin films were not successful, perhaps because of the hydrogen-rich reactant gases used for film depositions. It has been proposed that  $CH_3$  radicals (or  $C_2H_2$  molecules) are the growth species of diamond thin films in  $H_2$ -rich plasmas, with the growth surface terminated by atomic hydrogen. Consequently, if nitrogen atoms or CN radicals reach the growth surface during deposition, atomic hydrogen from the hydrogen-rich plasma can abstract the nitrogen from the growth surface to form NH, and then terminate dangling bonds with hydrogen. By contrast, in a nitrogen plasma,  $C_2$  appears to be the major growth species, and hydrogen abstraction reaction is not required for the growth with  $C_2$ ,<sup>20</sup> which may make the incorporation of nitrogen into diamond films possible.

It is well known that nitrogen is a deep donor impurity in diamond, resulting in a complex defect-related band structure with a high density of gap states. Based on photoluminescence (PL) and cathodoluminescence (CL) spectroscopy

measurements, the major nitrogen-related defect centers include a vacancy trapped at a substitutional nitrogen atom (1.94 eV), a vacancy and a nitrogen atom (2.15 eV), vacancies trapped at A centers (2.30 and 2.46 eV), vacancies trapped at nitrogen B centers (2.49 eV), and so on.<sup>23</sup> These nitrogen related defect centers may play an important role in enhancing electron field emission from the surface of the nanocrystalline diamond thin films, because without the nitrogen incorporation, the Fermi level of the diamond films is about 4.5 eV deep. Note that some planes of diamond have a negative electron affinity, meaning that the minimum energy state in vacuum is lower (about 0.7 eV) than the minimum energy state in the conduction band.<sup>24</sup> Consequently, the energy barrier between the nitrogen-related defect centers listed above and the minimum of the vacuum energy level will be reduced to 1.0–1.8 eV. As a result of reducing the surface energy barrier by nitrogen impurity or nitrogen related defects, electrons from the nitrogen donor states may more easily tunnel into vacuum under the influence of a local electric field. A detailed study of the microstructure and defect features of our nitrogen incorporated nanocrystalline diamond film is under way.

#### IV. CONCLUSION

Microwave plasma enhanced CVD with a mixture of  $N_2$  and  $CH_4$  as the reactant gas has been employed to synthesize nitrogen incorporated diamond thin film. X-ray powder diffraction, TEM, and EELS characterizations demonstrate that the films prepared from the  $N_2/CH_4$  plasma consist of a pure nanocrystalline diamond phase. High-resolution SIMS analysis shows that nitrogen with a concentration of  $8 \times 10^{20}$  atoms/cm<sup>3</sup> has been incorporated into the nanocrystalline diamond thin films when the reactant gas with 96 vol. %  $N_2$  and 4 vol. %  $CH_4$  has been used. Electron field emission measurements reveal that the onset field of the emission from the nitrogen incorporated nanocrystalline diamond films is about 3.2  $V/\mu m$ . It has been suggested that the electron gap states provided by the incorporated nitrogen play an important role of enhancing the electron field emission from the surface of the nanocrystalline thin film.

#### ACKNOWLEDGMENTS

The authors wish to thank C. D. Zuiker, H. Oechsner, and R. Csencsits for valuable discussions. The research reported here was conducted with support from the U.S. Department of Energy, Office of Basic Energy Science, under Contract No. W-31-109-ENG-38.

- <sup>1</sup>S. A. Kajihara, A. Antonelli, J. Bernholc, and R. Car, *Phys. Rev. Lett.* **66**, 2010 (1991).
- <sup>2</sup>R. G. Farrer, *Solid State Commun.* **7**, 685 (1969).
- <sup>3</sup>W. Kaiser and W. L. Bond, *Phys. Rev.* **115**, 857 (1959).
- <sup>4</sup>R. Berman, P. R. W. Hudson, and M. Martinez, *J. Phys.* **18**, 1430 (1975).
- <sup>5</sup>M. W. Geis, J. C. Twichell, J. Macaulay, and K. Okano, *Appl. Phys. Lett.* **67**, 1328 (1995).
- <sup>6</sup>K. Okano, S. Koizumi, S. R. P. Silva, and G. A. J. Amarantunga, *Nature (London)* **381**, 140 (1996).
- <sup>7</sup>J. Mort, M. A. Machonkin, and K. Okumura, *Appl. Phys. Lett.* **59**, 3148 (1991).

- <sup>8</sup>H. Spicka, M. Griesser, H. Hutter, M. Grasserbauer, S. Bohr, R. Haubner, and B. Lux, *Diam. Relat. Mater.* **5**, 383 (1996).
- <sup>9</sup>M. W. Geis, N. N. Efremow, J. D. Woodhouse, M. D. McAleese, M. Marchywka, D. G. Socker, and J. F. Hochedez, *IEEE Electron Device Lett.* **12**, 456 (1991).
- <sup>10</sup>C. Wang, A. Garcia, D. C. Ingram, M. Lake, and M. E. Kordes, *Electron. Lett.* **27**, 1459 (1991).
- <sup>11</sup>N. Kumar, H. K. Schmidt, and C. Xie, *Semicond. Sci. Technol.* **38**, 71 (1995).
- <sup>12</sup>W. Zhu, G. P. Kochanski, S. Jin, L. Seibles, D. C. Jacobson, M. McCormack, and A. E. White, *Appl. Phys. Lett.* **67**, 1157 (1995).
- <sup>13</sup>G. Popovici and M. A. Prelas, *Diam. Relat. Mater.* **4**, 1305 (1995).
- <sup>14</sup>A. Badzian, T. Badzian, and S.-T. Lee, *Appl. Phys. Lett.* **62**, 3432 (1993).
- <sup>15</sup>R. Locher, C. Wild, N. Herres, D. Behr, and P. Koidl, *Appl. Phys. Lett.* **65**, 34 (1994).
- <sup>16</sup>S. Jin and T. D. Moustakes, *Appl. Phys. Lett.* **65**, 403 (1994).
- <sup>17</sup>C. Wild, R. Kohl, N. Herres, W. Müller-Sebert, and P. Koidl, *Diam. Relat. Mater.* **3**, 373 (1994).
- <sup>18</sup>C. D. Zuiker, D. M. Gruen, and A. R. Krauss, *J. Appl. Phys.* **79**, 3541 (1996).
- <sup>19</sup>D. M. Gruen, S. Liu, A. R. Krauss, J. Luo, and X. Pan, *Appl. Phys. Lett.* **64**, 1502 (1994).
- <sup>20</sup>P. C. Redfern, D. A. Horner, A. A. Curtiss, and D. M. Gruen, *J. Phys. Chem.* **100**, 11654 (1996).
- <sup>21</sup>S. P. Smith and R. G. Wilson, in *Secondary Ion Mass Spectrometry SIMS VII*, edited by A. Benninghoven (Wiley, Chichester, 1990), p. 147.
- <sup>22</sup>R. H. Fowler and L. Nordheim, *Proc. R. Soc. London, Ser. A* **119**, 173 (1928).
- <sup>23</sup>W. Zhu, in *Diamond: Electronic Properties and Applications*, edited by L. S. Pan and D. R. Kania (Kluwer, Boston, 1995), pp. 200, 201.
- <sup>24</sup>M. W. Geis, J. C. Twichell, and T. M. Lyszczarz, *J. Vac. Sci. Technol. B* **14**, 2060 (1996).